

Temporal delays among place cells determine the frequency of population theta oscillations in the hippocampus

Caroline Geisler^{1,2}, Kamran Diba, Eva Pastalkova, Kenji Mizuseki, Sebastien Royer³, and György Buzsáki²

Center for Molecular and Behavioral Neuroscience, Rutgers University, Newark, NJ 07102

Edited* by Nancy J. Kopell, Boston University, Boston, MA, and approved March 5, 2010 (received for review October 29, 2009)

Driven either by external landmarks or by internal dynamics, hippocampal neurons form sequences of cell assemblies. The coordinated firing of these active cells is organized by the prominent “theta” oscillations in the local field potential (LFP): place cells discharge at progressively earlier theta phases as the rat crosses the respective place field (“phase precession”). The faster oscillation frequency of active neurons and the slower theta LFP, underlying phase precession, creates a paradox. How can faster oscillating neurons comprise a slower population oscillation, as reflected by the LFP? We built a mathematical model that allowed us to calculate the population activity analytically from experimentally derived parameters of the single neuron oscillation frequency, firing field size (duration), and the relationship between within-theta delays of place cell pairs and their distance representations (“compression”). The appropriate combination of these parameters generated a constant frequency population rhythm along the septo–temporal axis of the hippocampus, while allowing individual neurons to vary their oscillation frequency and field size. Our results suggest that the faster-than-theta oscillations of pyramidal cells are inherent and that phase precession is a result of the coordinated activity of temporally shifted cell assemblies, relative to the population activity, reflected by the LFP.

assembly sequence | cell assembly | phase precession | phase coding | ventral hippocampus

Neural oscillations detected in the local field potential (LFP) provide important information about the cooperative activity of neuronal populations (1–3). In the simplest case, the firing rate of a subset of neurons oscillates with a particular mean frequency, and this seed population functions as the pacemaker and biases the discharge phase of the remaining majority. Examples include the various rhythms of the thalamocortical system, where individual neurons fire strictly at a specific phase of the LFP (4). A similar scenario has been hypothesized to be realized in the hippocampal–entorhinal system, with the medial septum serving as the pacemaker of the prominent theta rhythm (5–10 Hz) (5, 6). However, hippocampal neurons in the exploring rat are active in short bouts, typically representing a particular place (7). During such high-firing epochs, place cells oscillate faster than the frequency of theta LFP (8–10), the result of which is a progressive phase precession of place cell spikes (8, 11). The frequency of the LFP theta is constant across the whole hippocampus, even though the size of place fields increases whereas the oscillation frequency of place cells decreases along the septo–temporal (dorsal–ventral) axis of the hippocampus (12–14). Furthermore, the LFP theta is highly coherent at different stages of the hippocampal–entorhinal loop (15–19).

The discrepancy between the oscillation frequencies of spiking place cells and the global rhythm reflected in the LFP led us to pose several questions. Given that the output of hippocampal pyramidal cells is in tune with their targets, how do phase precessing place cells generate a rhythmic activity at theta frequency? Furthermore, how does the neuronal coordination allow for large differences of place cell oscillation frequencies across the hippocampal regions? To address these questions, we designed

an analytical model and confronted the model predictions with experimentally derived parameters.

Results

All data were collected while the rats were running on various tracks (14, 19–21). Fig. 1*A* illustrates the spatial distribution and temporal course of spiking of example neurons recorded in a single session. Spikes of active place cells showed robust theta phase precession as the rat moved across the place field (Fig. 1*B* and *C*), and the oscillation frequency of individual place cells was faster than that of the simultaneously recorded LFP theta (Fig. 1*D*). As reported previously (9, 11, 20, 22, 23), the theta-scale time lag (τ) and the distance between the preferred locations of cell pairs were correlated (Fig. 1*E* and *F*). The linear part of the curve was confined to the temporal window of approximately a half theta period (*ca.* 60 ms), representing ≈ 50 cm distance (12, 20, 22). The distances between the place fields correlate with the time it takes for the rat to run between the place fields (“real” time; T in Fig. 1*E*). This relationship reflects an ≈ 20 -fold temporal compression, assuming a constant running speed of 50 cm/s.

Despite the systematic, position-dependent forward phase shift of spikes, the number of spikes fired by CA1 place cells per theta cycle increased then decreased as the rat traveled through the field (Fig. 1*B*), such that the highest firing rate occurs at the center of the place field, coinciding with the maximal firing at the trough of the LFP theta (Fig. 1*C* and Fig. S1; see also refs. 22, 24).

Assuming a constant locomotion velocity within and across trials, travel distances can be expressed in the time domain as travel durations. Only trials in which the rat ran in a continuous forward motion (minimal speed 10 cm/s) and the LFP was sufficiently theta modulated (see *Methods*) were included in the analysis. We characterized the activity of pyramidal cells using their oscillation frequencies f_0 , their relative frequencies with respect to the LFP theta f_0/f_θ , and their place-field sizes in seconds L . Further, the travel time between place fields T and the theta time scale time lag between place cell pairs τ are correlated, and their relationship defines the “compression factor” c (Fig. 2 and Fig. S2). These experimentally derived measures were subsequently used in the modeling section of this report (below). In the example session shown in Fig. 2, CA1 pyramidal cells during running in the maze and in the running-wheel

Author contributions: C.G. and G.B. designed research; C.G., K.D., E.P., K.M., and S.R. performed research; C.G. contributed new reagents/analytic tools; C.G., K.D., E.P., K.M., and S.R. analyzed data; and C.G. and G.B. wrote the paper.

The authors declare no conflict of interest.

*This Direct Submission article had a prearranged editor.

¹Present address: Center for Integrative Neuroscience, Universität Tübingen, 72076 Tübingen, Germany.

²To whom correspondence may be addressed. E-mail: buzaski@andromeda.rutgers.edu or caroline.geisler@cin.uni-tuebingen.de.

³Present address: Howard Hughes Medical Institute, Janelia Farm Research Campus, Ashburn, VA 20147.

This article contains supporting information online at www.pnas.org/cgi/content/full/0912478107/DCSupplemental.

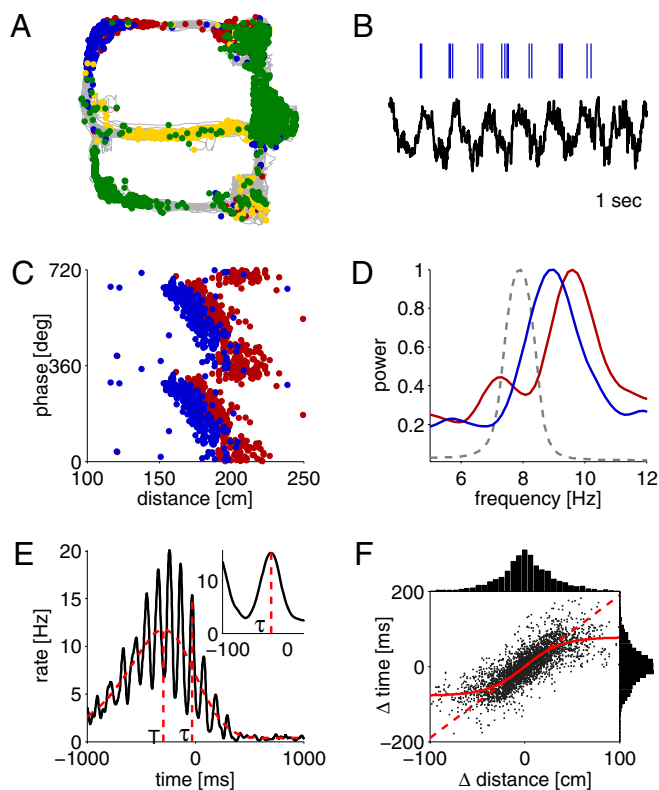


Fig. 1. Place cells oscillate faster than the theta LFP. (A) Example place cells active in different parts of the maze. Different colors correspond to the action potentials of different neurons. (B) Spiking activity of a neuron (blue ticks) and LFP in a single run (1 s is shown). (C) Rat's position in the maze (distance from the delay area) vs. theta phase demonstrates the precession of spiking phase for two neurons (red and blue, from A). (D) Power spectra (normalized) of unit firing (blue, peak power frequency 9 Hz; red, peak power frequency 9.6 Hz) and corresponding LFP (gray dashed line, peak power frequency 7.9 Hz). Note that the units oscillate faster than the LFP. (E) Temporal cross-correlation between the two place cells (red and blue in A, C, and D). Dashed line, smoothed rate of neuronal spiking to eliminate theta modulation. Temporal distance T is the time needed for the rat to run the distance between the peaks of the two place fields ($T = -295$ ms). Inset: τ is the distance between the first theta peak from zero and corresponds to the distance between the two neurons within the theta cycle ($\tau = -30$ ms). (F) Correlation between the peaks of place fields vs. theta-scale time lag τ for 3,352 pairs of neurons (data from ref. 20) is well fit by a sigmoid (red solid line) and by a linear fit in the central region (red dashed line; slope = 1.89 ms/cm). Top and Right: Histograms of distance and time lag, respectively.

were recorded in the same session (Fig. 2A and B). Note that both the LFP and pyramidal cells oscillate slower during wheel running than in the maze and that the firing fields L are longer in the wheel.

As a surrogate of direct measurement of phase precession of single cells, we calculated the relative oscillation frequencies of single neurons with respect to corresponding LFP segments (9, 19, 25). Overall, 84% of CA1 and 78% of CA3 pyramidal cells oscillated faster than the simultaneously recorded LFP theta (Fig. S3). Interneurons in general sustained a high and relatively stable firing rate during the run and oscillated at the same frequency as the LFP theta (but see refs. 9, 26).

Because nearly all active CA1 and CA3 pyramidal cells oscillated faster than the LFP, it is important to clarify how their population behavior relates to the LFP theta. Therefore, we analyzed not only the single unit activity but also the population output of place cells (POP) consisting of the combined spikes of the simultaneously recorded pyramidal cells. When sufficiently large numbers of pyramidal cells were active simultaneously in a given epoch (see also

Fig. S4), POP showed oscillatory fluctuations at the same frequency as the simultaneously recorded theta LFP (Fig. 3A–E and H). At the same time, individual pyramidal cells of the same population oscillated at a higher frequency than the LFP and the POP (Fig. 3F and G), indicating that the frequency of the global output of place cells is slower than that of the constituent neurons.

To understand better why the summed activity of neurons, reflected by the LFP, oscillates slower than the frequency of the individual cells, we built a firing rate–based model of a population of place cells that allows an analytical calculation of the model POP (mPOP). In the model shown in Fig. 4, each single place cell oscillates at 8.6 Hz for ≈ 1.5 s duration with increasing and decreasing rate/cycle to mimic the firing patterns of representative place cells in the dorsal hippocampus (see Methods and ref. 27). All model neurons are identical, and they cover together the entire “trial” interval (2 s) evenly. However, their oscillation cycles are shifted with respect to each other according to the compression factor $c = 0.075$, meaning that the time offset between the oscillatory cycles τ of the respective neurons depends on the time difference between the centers of their place fields T as $\tau = cT$ (as in Fig. 1E and Fig. 2). The model neurons form a chain of overlapping firing fields (Fig. 4A and B), and their summed activity produces an oscillation of constant amplitude A whose frequency, $f_\theta = 8$ Hz, is slower than the frequency of the individual model neurons (Fig. 4B). As a result of the phase interference between the faster single cells and the slower population oscillation, the phase between these two oscillators shows a systematic forward shift (phase precession), with the highest discharge probability at 180° (Fig. 4C and Eq. S2), corresponding to the trough of the theta cycle, as observed experimentally (Fig. S1).

We assume that the activity of place cells can be approximated by a sine wave of frequency f_0 multiplied by a Gaussian place field of width $\sigma = L/3\sqrt{2}$ and centered at time T (see Eq. 2). The population frequency f_θ and the oscillation amplitude A are calculated from the compression factor c , the single-cell oscillation frequency f_0 , and the place field size L (Eqs. 6 and 7 and Fig. S4). The oscillation frequency of the mPOP $f_\theta = f_0(1 - c)$ (Eq. 7) is directly linked to the delays between the individually oscillating place cells, represented by the compression factor c . The oscillation amplitude is $A = e^{-(\pi c L / (3\sqrt{2} f_0))^2}$ (Eq. 6 and Eq. S1) and goes to zero for infinitely large place fields (corresponding to large L), with fixed single cell oscillation frequency f_0 and compression factor c , because the phase-shifted oscillators average each other out. Furthermore, the phase shift between the oscillation of the single place cell and mPOP at the center of the place field (T_n) is always zero (Eq. S2), corresponding to the trough of LFP theta. The population frequency can be written as $f_\theta = f_0 - 1/L$ (Eq. 8 and Fig. S5), and the amplitude is a constant (Eq. S7), if we constrain the size of the place field to 360° phase precession (refs. 8, 28; but see Fig. S6).

Using measured parameters from experiments (e.g., f_0 , c , and L), we predicted other experimental parameters (e.g., f_θ) with the model. There is an excellent agreement between the model (using Eq. 7) and experiment in both the examples (compare Figs. 2 and 5) and in 14 additional sessions in which sufficiently large numbers of neurons were available for the estimation of the compression factor (Fig. 6A). In additional sessions in which c could not be directly measured, it was estimated from the relationship between firing field size L and the oscillation frequency f_0 (Eq. 9). The prediction of the model agreed well with the experimental observations for these 680 neurons (Fig. 6B–E).

Up until now, we assumed in the model that the place field size and single neuron oscillation frequency were relatively uniform. However, the place field size can be very variable within the dorsal hippocampus, and the mean place field size increases along the septo–temporal axis, parallel with a decreased oscillation frequency of place cells (12–15, 18). How can a population of neurons, which differ in oscillation frequency, place field size, and temporal offsets generate a coherent theta frequency population output? To allow

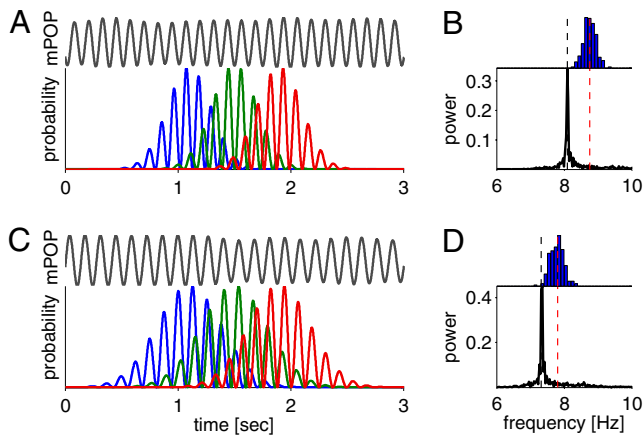


Fig. 5. Modeling the population output of model place cells (mPOP) on the basis of experimental data from Fig. 2. (A) Using the experimentally derived parameters during track running (mean frequency of single neurons $f_0 = 8.61$ Hz, compression factor $c = 0.075$, and firing field size $L = 1.5$ s), the oscillation frequency of the population output of the model place cells is $f_\theta = 7.97$ Hz (compare with the measured LFP frequency $f_\theta = 8.09$ Hz). (B) Histogram shows the distribution of single unit oscillation frequencies above the power spectrum of the population activity mPOP shown in A. Red dashed line, mean frequency of single neurons; black dashed line, peak frequency of mPOP. (C) Same as in A, using experimentally derived parameters from wheel running ($f_0 = 7.71$ Hz, $c = 0.059$, $L = 2.15$ s). (D) The oscillation frequency of the mPOP ($f_\theta = 7.25$ Hz, compare with the measured LFP frequency $f_\theta = 7.32$ Hz) is much lower than the mean frequency of single neurons (red dashed line).

Cell Assembly Model of Theta Dynamics. Our model provides a framework for understanding the principles that support the temporal organization of single-cell and population dynamics in the hippocampus. The main assumptions of the model are that (i) the

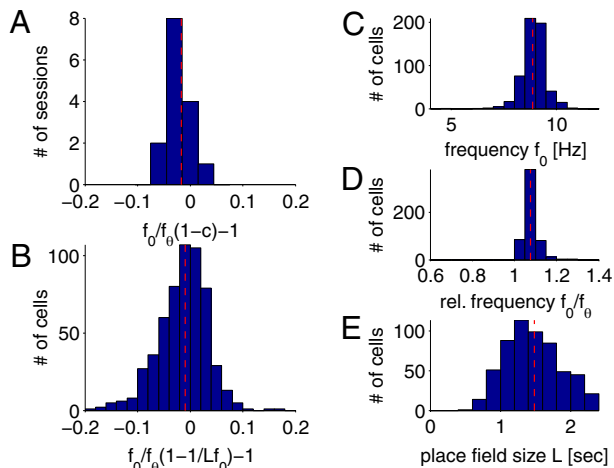


Fig. 6. Comparison between model predictions and experimental observations. (A) Histogram of the relative error between the relative average frequency predicted from the experimentally measured compression factor $(1 - c)$ and the relative frequency f_0/f_θ , averaged over the respective session. The mean error (red dashed line) is -0.017 (corresponding to $>98\%$ accuracy) for 16 recording sessions. (B) Histogram of the relative error between the relative frequency predicted from the place field size and the single neuron frequency $[1 - 1/(L f_0)]$, and the measured relative neuron frequency f_0/f_θ for 680 pyramidal cells. The relative mean error (red dashed line) is -0.0097 (corresponding to $>99\%$ accuracy). (C) Histogram of single neuron frequencies f_0 (red dashed line, mean frequency 8.85 Hz), (D) relative frequencies f_0/f_θ (red dashed line, mean relative frequency 1.07 Hz), and (E) place field size L (red dashed line, mean place field size 1.48 s) for 680 pyramidal cells.

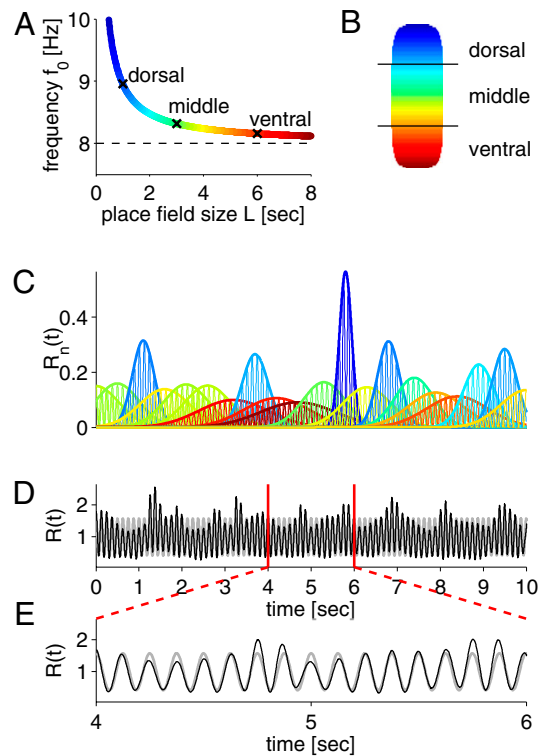


Fig. 7. Modeling the coherent theta frequency oscillations along the septo-temporal (dorsal-ventral) axis of the hippocampus. Pyramidal cells across the whole hippocampus oscillate at different frequencies, but their mPOP synchronizes at theta frequency. (A) The oscillation frequency f_0 decreases and the place field size L increases along the dorsal-ventral axis according to $f_0 = f_\theta - 1/L$, whereas the oscillation frequency of the mPOP does not change ($f_\theta = 8$ Hz). (B) Scheme of the hippocampus, color coded for decreasing oscillation frequencies of place cells, along the dorsal-ventral axis. (C) Firing fields of 20 selected place neurons, color coded to indicate their anatomical location in the dorsal-ventral axis (see B). (D) mPOP of 100 model pyramidal cells with randomly chosen oscillation frequencies (black line) and the analytically predicted 8 Hz population oscillation (gray line). (E) Enlargement of the traces of D. Note that the oscillation frequency of both lines is the same.

activity of a single cell can be approximated by a sine wave with a Gaussian envelope, (ii) the temporal distance between firing fields (T) and the temporal offset between the spikes of the respective neurons within the theta cycle (τ) are linked through the sequence compression factor (c) as $c = \tau/T$, (iii) the extent of phase precession ($\Delta\Phi$) is the same for all neurons (set here as 360° , but see Fig. S6), and (iv) the density of place cells is sufficiently high (Fig. S7). On the basis of these assumptions, we derived a relationship between the single neuron oscillation frequency (f_0), population oscillation frequency (f_θ), and the firing field size (L). All these relationships could be correctly predicted from parameters derived from data. If model neurons with identical firing field size and oscillation frequency were connected with random time delays, the amplitude of population fluctuation (i.e., theta oscillation) would converge to zero. However, assuming that the various parameters are controlled by interrelated physiological mechanisms, it is perhaps not surprising that the experimentally measured parameters have a mathematically definable relationship.

A fundamental assumption of the model is that single-cell parameters and their interactions, namely oscillation frequency of the single cell f_0 , the place fields size L , and the time delay between the oscillation cycles of pairs of place cells τ , need to be dynamically adjusted to support a coherently oscillating mPOP in the entire hippocampus (15, 12, 18, 13, 19). The three key parameters (f_0 , L , and τ) are “built-in”

parameters in the model without currently known physiological solutions. We hypothesize that the delays between sequentially active place cells is brought about by feed-forward inhibition. Faster spiking/oscillating cells can recruit stronger feed-forward inhibition, inducing longer delays and, consequently, a larger difference between the oscillation frequency of the constituent neurons and the population. The mechanisms that determine the duration (“lifetime”) of activity of place cells are not known either. Short-term synaptic plasticity and spiking-dependent adjustment of spike threshold (29, 30) are potential candidates for controlling the lifetime of place cells on theoretical grounds because they operate at the time scale of seconds (31–34). Our model does not address the origin of single neuron oscillation. Oscillatory activity may be a response to a pacemaker input, such as the medial septum (5, 35, 6, 36, 37), or may represent a locally emerging network phenomenon (38–42). However, neither pacemaker nor network models explain why active neurons, such as place cells, fire only transiently and at a frequency faster than the pacing or population rhythm. Therefore, we hypothesize that the oscillation of single neurons is a consequence of the same dynamic mechanisms that are also responsible for the phase delays, the finite size of place fields, and the global theta oscillations.

An intuitive explanation for the inverse relationship between the oscillation frequency of place cells and the firing field size is that larger deviations from the population oscillation frequency are less “tolerated” by the network than small differences, and therefore the activity of faster oscillating neurons is terminated sooner by stronger synaptic depression. According to the model, place cells with very large firing fields should oscillate at frequencies close to the POP (as reflected by the LFP theta) and with very small temporal offsets between the neurons (13, 14). Furthermore, pyramidal neurons perfectly phase-locked to the population oscillation should have infinitely large place fields. In support of this model prediction, pyramidal cells sustain prolonged spiking activity at a particular theta phase while the rat is running in a wheel without memory requirement (43, 44, 21). Current phase precession models explicitly assume that phase interference occurs between two independent oscillatory mechanisms, for example between single neurons and a pacemaker input (45–49, 10, 50). Our model does not require a reference pacemaker. Phase precession of single neurons emerges even if all constituent neurons have the same frequency and firing field size (Fig. 5), and results from the difference between the oscillation frequency of single neurons and their population output. Thus, there is a bidirectional relationship between single cells and their cooperative product: activity of single cells gives rise to a population rhythm, which in turn competes with the faster firing constituents by limiting their duration of activity.

Contribution of Place Cells to LFP Theta. How do transiently active, faster oscillating place cells contribute to the LFP theta? We have demonstrated in both experiment and model that the summed spikes of the active neurons yield a population output slower than the mean oscillation frequency of the constituent neurons. It follows that, for example, the CA3 population output can generate an 8-Hz rhythmic sink in the stratum radiatum of CA1 even if all CA3 place cells individually oscillate faster than 8 Hz. Similarly, the population effect of layer II grid cells (51) under the same behavioral conditions should also be 8 Hz, even though grid cells also show phase precession and thus oscillate faster than the population rhythm (10, 52, 25, 19). We predict that the relationships between the single neuron oscillation frequency (f_0), grid size (L), and temporal delays (τ) defined through the compression factor (c) also apply to neurons of the entorhinal cortex.

Methods

Experimental procedures, data acquisition, and analyses are described in *SI Methods*, available online.

Compression Factor. The “sequence compression” has been defined as the ratio between the pairwise time lag of place cells firing within one theta cycle and the distance between the centers of the respective place fields (11, 22, 9, 20). Under the assumption of constant running speed, we define here the “sequence compression factor” as the ratio between the time lag τ of firing within one theta cycle and the time T it takes the animal to run between the respective place fields in the environment (see also Fig. 1E):

$$c = \frac{\tau}{T} = \frac{\tau}{d} \cdot s. \quad [1]$$

where d = distance between place fields and s = running speed. The compression factor c is defined for a population of neurons and is generally nonzero.

Population Rate. N place fields are evenly distributed along a time interval T_N , and each place field is associated with one place cell. The discharge probability of the n th place cell is approximated by the product of a sine-wave of frequency f_0 and a Gaussian of width σ :

$$R_n(t) = [1 + e^{i2\pi f_0(t - \tau_n)}] \frac{1}{\sqrt{\pi}\sigma} e^{-(t - T_n)^2/\sigma^2} \quad [2]$$

where τ_n is the theta time lag, and T_n is the time of the center of the place field, both times are with respect to a chosen origin. The Gaussian is normalized to an integral of unity.

The rate of the population output of place cells (mPOP) is the sum of Eq. 2 over all neurons n :

$$R(t) = \frac{1}{\sqrt{\pi}\sigma} \frac{1}{\delta} \sum_n [1 + e^{i2\pi f_0(t - \tau_n)}] e^{-(t - T_n)^2/\sigma^2} \quad [3]$$

where δ is the cell density with $\delta = 1/\Delta T = c/\Delta\tau$, where $\Delta x = x_k - x_{k-1}$, $x = \{T, \tau\}$, $k = \{2, \dots, N\}$. In the limit of continuous variable $\lim_{\Delta\tau \rightarrow 0}$ and substituting $T_n = \tau_n/c \rightarrow \tau/c$ (see Eq. 1) the population rate (Eq. 3) can be written as:

$$R(t) = \frac{1}{\sqrt{\pi}\sigma c} \int_{-\infty}^{\infty} d\tau e^{-(\tau - ct)^2/(c\sigma)^2} + \frac{1}{\sqrt{\pi}\sigma c} \int_{-\infty}^{\infty} d\tau e^{-i2\pi f_0(\tau - t)} e^{-(\tau - ct)^2/(c\sigma)^2}. \quad [4]$$

Eq. 4 can be solved exactly:

$$R(t) = 1 + \frac{1}{\sqrt{\pi}\sigma c} e^{i2\pi f_0 t(1-c)} \times \int_{-\infty}^{\infty} d\tau e^{-i2\pi f_0(\tau - ct)} e^{-(\tau - ct)^2/(c\sigma)^2} = 1 + e^{i2\pi f_0(1-c)t} e^{-(\pi c \sigma f_0)^2} \quad [5]$$

The population rate (Eq. 5) describes an oscillation with unit mean, an oscillation amplitude

$$A(c, \sigma, f_0) \equiv e^{-(\pi c \sigma f_0)^2} \quad [6]$$

and an oscillation frequency

$$f_\theta \equiv f_0(1 - c). \quad [7]$$

Under the assumption that the total phase precession interval $\Delta\Phi = 360^\circ$ (see also *SI Methods*), the oscillation frequency is

$$f_\theta = f_0 - \frac{1}{L} \quad [8]$$

where L is the place field size, implying that

$$cL f_0 = 1. \quad [9]$$

ACKNOWLEDGMENTS. We thank Asohan Amarasingham, Horacio Rotstein, and Anton Sirota for comments and helpful discussions. This work was supported by National Institutes of Health Grants NS34994 and MH54671, National Science Foundation Grant SBE 0542013, and by the James S. McDonnell Foundation.

1. Friston KJ (2000) The labile brain. I. Neuronal transients and nonlinear coupling. *Philos Trans R Soc Lond B Biol Sci* 355:215–236.
2. Logothetis NK (2003) The underpinnings of the BOLD functional magnetic resonance imaging signal. *J Neurosci* 23:3963–3971.
3. Buzsáki G, Draguhn A (2004) Neuronal oscillations in cortical networks. *Science* 304:1926–1929.
4. Steriade M, McCormick DA, Sejnowski TJ (1993) Thalamocortical oscillations in the sleeping and aroused brain. *Science* 262:679–685.
5. Petsche H, Stumpf C, Gogolak G (1962) [The significance of the rabbit's septum as a relay station between the midbrain and the hippocampus. I. The control of hippocampal arousal activity by the septum cells]. *Electroencephalogr Clin Neurophysiol* 14:202–211.
6. Stewart M, Fox SE (1990) Firing relations of lateral septal neurons to the hippocampal theta rhythm in urethane anesthetized rats. *Exp Brain Res* 79:92–96.
7. O'Keefe J, Nadel L (1978) *The Hippocampus as a Cognitive Map* (Oxford Univ Press, London).
8. O'Keefe J, Recce ML (1993) Phase relationship between hippocampal place units and the EEG theta rhythm. *Hippocampus* 3:317–330.
9. Geisler C, Robbe D, Zugaro M, Sirota A, Buzsáki G (2007) Hippocampal place cell assemblies are speed-controlled oscillators. *Proc Natl Acad Sci USA* 104:8149–8154.
10. Burgess N, Barry C, O'Keefe J (2007) An oscillatory interference model of grid cell firing. *Hippocampus* 17:801–812.
11. Skaggs WE, McNaughton BL, Wilson MA, Barnes CA (1996) Theta phase precession in hippocampal neuronal populations and the compression of temporal sequences. *Hippocampus* 6:149–172.
12. Maurer AP, Vanrhoads SR, Sutherland GR, Lipa P, McNaughton BL (2005) Self-motion and the origin of differential spatial scaling along the septo-temporal axis of the hippocampus. *Hippocampus* 15:841–852.
13. Kjelstrup KB, et al. (2008) Finite scale of spatial representation in the hippocampus. *Science* 321:140–143.
14. Royer S, Sirota A, Patel J, Buzsáki G (2010) Distinct representations and theta dynamics in dorsal and ventral hippocampus. *J Neurosci* 30:1777–1787.
15. Bullock TH, Buzsáki G, McClune MC (1990) Coherence of compound field potentials reveals discontinuities in the CA1-subiculum of the hippocampus in freely-moving rats. *Neuroscience* 38:609–619.
16. Mitchell SJ, Ranck JB, Jr (1980) Generation of the theta rhythm in medial entorhinal cortex of freely moving rats. *Brain Res* 189:49–66.
17. Chrobak JJ, Buzsáki G (1998) Operational dynamics in the hippocampal-entorhinal axis. *Neurosci Biobehav Rev* 22:303–310.
18. Lubenov EV, Siapas AG (2009) Hippocampal theta oscillations are travelling waves. *Nature* 459:534–539.
19. Mizuseki K, Sirota A, Pastalkova E, Buzsáki G (2009) Theta oscillations provide temporal windows for local circuit computation in the entorhinal-hippocampal loop. *Neuron* 64:267–280.
20. Diba K, Buzsáki G (2008) Hippocampal network dynamics constrain the time lag between pyramidal cells across modified environments. *J Neurosci* 28:13448–13456.
21. Pastalkova E, Itskov V, Amarasingham A, Buzsáki G (2008) Internally generated cell assembly sequences in the rat hippocampus. *Science* 321:1322–1327.
22. Dragoi G, Buzsáki G (2006) Temporal encoding of place sequences by hippocampal cell assemblies. *Neuron* 50:145–157.
23. Ego-Stengel V, Wilson MA (2007) Spatial selectivity and theta phase precession in CA1 interneurons. *Hippocampus* 17:161–174.
24. Huxter J, Burgess N, O'Keefe J (2003) Independent rate and temporal coding in hippocampal pyramidal cells. *Nature* 425:828–832.
25. Jeewajee A, Barry C, O'Keefe J, Burgess N (2008) Grid cells and theta as oscillatory interference: Electrophysiological data from freely moving rats. *Hippocampus* 18:1175–1185.
26. Maurer AP, Cowen SL, Burke SN, Barnes CA, McNaughton BL (2006) Phase precession in hippocampal interneurons showing strong functional coupling to individual pyramidal cells. *J Neurosci* 26:13485–13492.
27. Samsonovich A, McNaughton BL (1997) Path integration and cognitive mapping in a continuous attractor neural network model. *J Neurosci* 17:5900–5920.
28. Maurer AP, Cowen SL, Burke SN, Barnes CA, McNaughton BL (2006) Organization of hippocampal cell assemblies based on theta phase precession. *Hippocampus* 16:785–794.
29. Sprunt N, Schiller Y, Stuart G, Sakmann B (1995) Activity-dependent action potential invasion and calcium influx into hippocampal CA1 dendrites. *Science* 268:297–300.
30. Henze DA, Buzsáki G (2001) Action potential threshold of hippocampal pyramidal cells in vivo is increased by recent spiking activity. *Neuroscience* 105:121–130.
31. Abbott LF, Regehr WG (2004) Synaptic computation. *Nature* 431:796–803.
32. Mongillo G, Barak O, Tsodyks M (2008) Synaptic theory of working memory. *Science* 319:1543–1546.
33. Fujisawa S, Amarasingham A, Harrison MT, Buzsáki G (2008) Behavior-dependent short-term assembly dynamics in the medial prefrontal cortex. *Nat Neurosci* 11:823–833.
34. Buonomano DV, Maass W (2009) State-dependent computations: Spatiotemporal processing in cortical networks. *Nat Rev Neurosci* 10:113–125.
35. Bland BH (1986) The physiology and pharmacology of hippocampal formation theta rhythms. *Prog Neurobiol* 26:1–54.
36. Lee MG, Chrobak JJ, Sik A, Wiley RG, Buzsáki G (1994) Hippocampal theta activity following selective lesion of the septal cholinergic system. *Neuroscience* 62:1033–1047.
37. Wang XJ (2002) Pacemaker neurons for the theta rhythm and their synchronization in the septohippocampal reciprocal loop. *J Neurophysiol* 87:889–900.
38. Konopacki J, MacIver MB, Bland BH, Roth SH (1987) Carbachol-induced EEG 'theta' activity in hippocampal brain slices. *Brain Res* 405:196–198.
39. Bland BH, Colom LV, Konopacki J, Roth SH (1988) Intracellular records of carbachol-induced theta rhythm in hippocampal slices. *Brain Res* 447:364–368.
40. Kocsis B, Bragin A, Buzsáki G (1999) Interdependence of multiple theta generators in the hippocampus: A partial coherence analysis. *J Neurosci* 19:6200–6212.
41. Gillies MJ, et al. (2002) A model of atropine-resistant theta oscillations in rat hippocampal area CA1. *J Physiol* 543:779–793.
42. Rotstein HG, et al. (2005) Slow and fast inhibition and an H-current interact to create a theta rhythm in a model of CA1 interneuron network. *J Neurophysiol* 94:1509–1518.
43. Czurkó A, Hirase H, Csicsvari J, Buzsáki G (1999) Sustained activation of hippocampal pyramidal cells by 'space clamping' in a running wheel. *Eur J Neurosci* 11:344–352.
44. Hirase H, Czurkó A, Csicsvari J, Buzsáki G (1999) Firing rate and theta-phase coding by hippocampal pyramidal neurons during 'space clamping'. *Eur J Neurosci* 11:4373–4380.
45. Kamondi A, Acsády L, Wang XJ, Buzsáki G (1998) Theta oscillations in somata and dendrites of hippocampal pyramidal cells in vivo: Activity-dependent phase-precession of action potentials. *Hippocampus* 8:244–261.
46. Magee JC (2001) Dendritic mechanisms of phase precession in hippocampal CA1 pyramidal neurons. *J Neurophysiol* 86:528–532.
47. Mehta MR, Lee AK, Wilson MA (2002) Role of experience and oscillations in transforming a rate code into a temporal code. *Nature* 417:741–746.
48. Harris KD, Csicsvari J, Hirase H, Dragoi G, Buzsáki G (2003) Organization of cell assemblies in the hippocampus. *Nature* 424:552–556.
49. Lengyel M, Szatmáry Z, Erdi P (2003) Dynamically detuned oscillations account for the coupled rate and temporal code of place cell firing. *Hippocampus* 13:700–714.
50. Harvey CD, Collman F, Dombeck DA, Tank DW (2009) Intracellular dynamics of hippocampal place cells during virtual navigation. *Nature* 461:941–946.
51. Hafting T, Fyhn M, Molden S, Moser MB, Moser EI (2005) Microstructure of a spatial map in the entorhinal cortex. *Nature* 436:801–806.
52. Hafting T, Fyhn M, Bonnevie T, Moser MB, Moser EI (2008) Hippocampus-independent phase precession in entorhinal grid cells. *Nature* 453:1248–1252.